9) Liaw, C. H., J. S. P. Wang, R. A. Greenkorn and K. C. Chao: *AIChE J.*, **25**, 376 (1979).
10) Moon, H. and W. K. Lee: *J. Colloid and Interface Sci.*, **96**, 162 (1983).
11) Neretnieks, I.: *Chem. Eng. Sci.*, **31**, 107 (1976).
12) Peel, R. G. and A. Benedek: *Cana. J. Chem. Eng.*, **59**, 688 (1981).
13) Sudo, Y., D. M. Misic and M. Suzuki: *Chem. Eng. Sci.*, **33**, 1287 (1978).
14) Suzuki, M. and T. Fujii: *AIChE J.*, **28**, 380 (1982).
15) Vermeulen, T.: *I.E.C.*, **45**, 1664 (1953).
16) Villadsen, B. A. and M. L. Michelsen: "Solution of Differential Equation Models by Polynominal Approximation," Prentice Hall, New York (1978).

PATTERN RECOGNITION IN FLOW VISUALIZATION AROUND A PADDLE IMPELLER

SUGENG WINARDI, SHUYA NAKAO AND YOICHI NAGASE
Department of Chemical Engineering, Hiroshima University, Higashi-Hiroshima 724

Key Words: Mixing, Paddle Impeller, Visualization, Flow Recognition, Impeller Stream, Conditional Sampling, Velocity Distributions, Torque Fluctuations

Very low frequency fluctuations in the velocity signal from several seconds to several minutes in scale are usually observed in agitated vessels. It is shown in this work that these fluctuations result from the abrupt replacement of the flow pattern in the vessel, even in part. Pattern recognition studies of the flow in the impeller region of a paddle were carried out, using high-speed VTR. The results showed that the flow between blades is characterized into five patterns which are replaced one after another. They are classified into the discharge and the cross-pass types of flow. The latter means that flow passes between impeller blades, upwardly or downwardly. The lifetime of the discharge flow type was three times that of the cross-pass flow type. The velocity distributions of the discharge and cross-pass flow types estimated from visualized pictures were quite different from each other and were different from the average distributions obtained by LDV. When the cross-pass pattern had developed over the whole region between blades, a horizontal figure-eight pattern of flow developed in the entire vessel with abrupt reduction of the torque.

Introduction

Most measurements of turbulence in a mixing vessel have shown that the relative intensities were higher than 50%.[2,3,7,9,13-15] Rao and Brodkey[13] pointed out that a flat-blade impeller caused random movement of the impeller stream. Mujumdar *et al.*[7] and Gunkel *et al.*[3] attempted to separate the velocity fluctuations into random and periodic components. Van't Riet and Smith[16] found a trailing vortex that originated in the region behind the upper and lower edges of the blade of the turbine impeller. They introduced the pseudo-turbulence concept, which is that most of the velocity fluctuations detected by a stationary probe in the discharge stream are largely dependent on the trailing vortex.[17] Subsequent works have extensively investigated the trailing vortex flow.[1,5,6,15] Recently, Yianneskis *et al.*[18] determined experimentally the structure of the trailing vortex produced by a disc turbine, using LDV technique. However, there are a few measurements of the discharge flow from a paddle impeller. One of the present authors found cross-pass flow, in which flow passes axially through the region between the blades of the paddle, together with the usual discharge flow.[9,10] A similar observation was reported by Oldshue.[12] Thus the real flow in the vessel is very unstable in the sense of the combination of the cross-pass patterns and the discharge patterns including trailing vortex. In fact, the flow in the vessel could be said to be a kind of unstable turbulent flow, in that several kinds of turbulent flows are distributed in the vessel locally at the same time, and the distribution changes continuously with time.

The paddle impeller is more often used in practice than the turbine impeller. Therefore, for further advancement of mixing research it is interesting to recognize unstable turbulent flow phenomena in the vessel before making a turbulence analysis. This work is a first attempt at flow recognition as a means of on simplifying the study of the real flow.

Received September 16, 1987. Correspondence concerning this article should be addressed to S. Winardi.

1. Experimental Apparatus

A paddle impeller with four blades was used in a baffled vessel. The experimental apparatus and its dimensions are shown in **Fig. 1**. The mixing vessel, made of transparent acrylic resin, was placed in a square glass tank filled with the same liquid as in the vessel in order to eliminate optical distortion. The impeller was located at half the liquid height. The impeller rotational speed was held constant at 120 rpm. Polyethylene particles approximately 2 mm in diameter were used as tracer. Their density was adjusted to be nearly equal to that of water by coating with white paint.

The flow visualization technique was very useful for the present purpose, and was improved greatly by use of a high-speed VTR system (NAC, HSV-200) with maximum framing speed of 200 fields per second. Visualizations were carried out in the impeller region between blades or in the whole vessel through bottom view or side view, using the high-speed VTR system. To obtain stereoscopic images of flow, simultaneous recording of side and bottom views was attempted using a regular VTR system together with the high-speed VTR system. Human observation at the other side of the vessel was also carried out along with simultaneous recording by the two VTRs to train the human judgement in the flow patterns on the VTR pictures. Remarks were recorded on the audio channel of the VTR system when replacement of the flow pattern was observed. The results of oral and video tape records were checked with each other. The training was repeated over a long time in order to obtain detailed and exact recognition of the flow patterns.

Torque measurement was also carried out together with the visualization.

2. Results and Discussion

2.1 Recognition of flow patterns in the impeller region

The flow between blades is complex, three-dimensional turbulent flow. The objective of this work is to point out that the complexity comes in part from the complete change of flow pattern from one type to the other, alternately, on a large time scale. Quantitative confirmation of this pattern replacement requires three-dimensional measurement at multiple points. Flow visualization is only method by which the authors could achieve the present objective. Efforts were concentrated on minimizing the artificiality of pattern recognition in training the investigators as described above. The flow patterns identified were as follows:

1. Pattern TD—pattern of high-speed radial discharge flow including violent trailing vortex as shown in **Fig. 2(a)**.

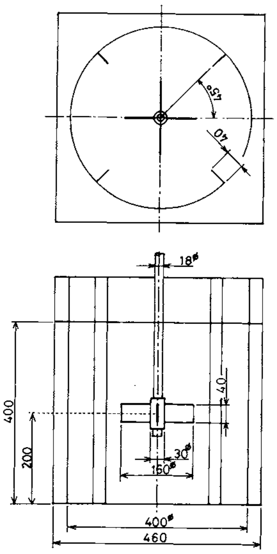

Fig. 1. Experimental apparatus

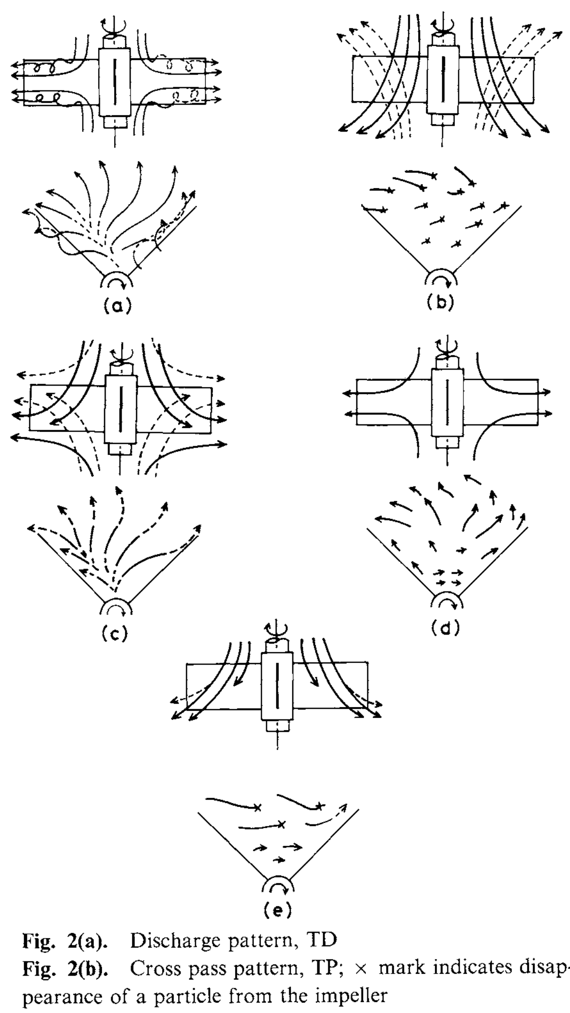

Fig. 2(a). Discharge pattern, TD
Fig. 2(b). Cross pass pattern, TP; × mark indicates disappearance of a particle from the impeller
Fig. 2(c). Asymmetric Discharge pattern, UD
Fig. 2(d). Illustration of Weak Discharge pattern, WD
Fig. 2(e). Illustration of Weak Cross-pass pattern, WP

2. Pattern TP—cross-pass flow pattern as shown in Fig. 2(b). The flow between blades is occupied completely by an intensive stream which passes between blades axially.

3. Pattern UD—asymmetric discharge flow pattern as shown in Fig. 2(c). The flow in the region between blades is directed radially, but the flow is asymmetric with respect to the horizontal plane of the impeller, $z=0$. The stream is intensive.

4. Pattern WD—weak discharge flow pattern as shown in Fig. 2(d). The fluid between blades streams out radially at low velocity as a whole. No trailing vortex is found in this pattern.

5. Pattern WP—weak cross-pass flow pattern as shown in Fig. 2(e). It is similar to pattern TP but is at low velocity as a whole.

One of the authors[9,11] estimated that the trailing vortex could maintain most of the angular momentum transferred from the impeller to the surrounding fluid, and that a high-speed radial discharge stream was induced at the time that the trailing vortex was generated. The latter was confirmed in this work on analyzing the high-speed VTR visualization. A photographic example of pattern TD was given by van't Riet *et al.*[16] Identification of pattern TP is the flow that turns in a radial direction after passing through the impeller region upward or downward. A photographic example of pattern TP was given by Oldshue.[12] Patterns TD and TP can be identified by anyone who observes the VTR pictures.

It should be recognized that pattern UD is not a combination of patterns TD and TP. Pattern UD is not a transition state between patterns TD and TP, but is an independent flow pattern which occurs following every type of pattern. Besides patterns TD, TP and UD, there were many possibilities of flow patterns in the VTR pictures. The discharge velocities of these patterns were lower as a whole than those of patterns TD, TP and UD. In addition, most were classified into weak discharge flow patterns or weak cross-pass flow patterns. Then they were identified as pattern WD and WP in this study. Patterns WD and WP included not only a flow similar to Figs. 2(d) and 2(e), but also a flow which was disturbed by the vertical vortex located near the blade tip, and a flow a part of which streamed oppositely in a radial direction (back-flow) and so on. Therefore, personal errors in recognition of patterns WD and WP are inevitable.

Some quantitative results of recognition will be given hereafter for pictures taken over a ten-minute period.

It is interesting to see the generation ratio and lifetime of each flow pattern. Table 1 shows the ratio of average lifetime of each pattern in the impeller region. The ratio is defined as (total lifetime of one pattern during ten minutes)/(ten minutes $\times 4$). The lifetime ratio of the cross-pass flow patterns, (patterns TP plus WP) is about one-quarter of the total time. The probability of pattern TP is the same as that of pattern UD, which is approximately 10%, while pattern TD reaches 35%.

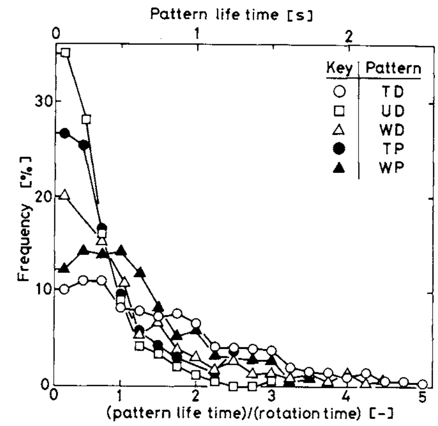

Fig. 3. Lifetime distributions of respective patterns

Table 1. Frequency of each pattern

Pattern	Ratio of average lifetime	
TD		34.9%
UD		9.9%
WD		29.6%
	Total	74.4%
TP		9.6%
WP		16.0%
	Total	25.6%

Lifetime distributions of each pattern are shown in **Fig. 3**. In the figure, the continuous VTR picture was divided into the interval of one-fourth rotation of the impeller blade. Within this time interval, major flow pattern between blades was judged and the frequency was calculated. Then, the ordinate means frequency per one-fourth rotation. Abscissa is non-dimensionalized by one rotation time of the impeller, which is 0.5 second in this experiment. It can be seen that the lifetime of the pattern TD is longer than the others, and the lifetime of TP and UD are short. Comparing these results with **Table 1**, it is indicated that, for example, the pattern TD has longer lifetime with lower generation frequency relative to the pattern WD, while WD has relatively short lifetime with high generation frequency. Patterns UD and TP have shorter lifetime and lower generation frequency than those of patterns TD, WD and WP.

It is also interesting to see the pattern combinations occurred simultaneously in the entire impeller region, four space between blades. Same pictures analized in Fig. 3 were again divided into one-fourth rotation and were recognized for the pattern combinations within that interval. The result is given in Table 2. It is noticed that the possibilities of patterns TD and TP occurred simultaneously in the entire space are only 9.3 and 0.6%. However, sum of pattern combinations of the discharge flow type which is shown in part (I) reaches 62%. While sum of part (II), combinations of the cross-pass flow type, is 15 percent. Ratio of them is 4 : 1. Dominant pattern in the item of "other combinations of TD, UD and WD" is pattern WD. Part (III) shows possibilities of coexisting of the discharge pattern together with cross-pass pattern in which at least one space between blades includes intense flow, that is TD, UD and TP. Sum of part (III) is almost equal to that of part (II).

2.2 Velocity distributions around the impeller

Results in the foregoing paragraph suggest that if one carries out the usual analysis for the turbulent signal, available informations are difficult to be deduced. An example will be seen in **Fig. 4**. Curves in the figure were determined as follows.

After the conditional sampling of the VTR pictures for four minutes, patterns TP, WP and UD were rearranged into the upward and downward cross-pass flow types. Patterns TD and WD were summed up to the discharge flow type. Then, pictures were classified to the discharge, upward and downward flow types. One thousand or more particle trajectories near the each planes AA′, BB′ and A′B′ were acquired from each of above three flow types. Then, velocities were calculated from the movements of tracer particles, and were smoothed applying the spline function to deduce velocity distributions. Those distributions for the discharge, upward and downward flow types are shown in Fig. 4 on two dotted and dashed lines, dotted and dashed lines and dashed lines, respectively. Downward flow type, for example, shows large velocity on plane BB′, since it is sum of inlet flow on planes AA′ and A′B′. That dashed line on plane A′B′ changes from inlet flow (negative) to outlet (positive) means a part of downward flow passes the lower part of the blade tip to the right downward direction which mainly comes from the pattern UD. Velocity distribution of the discharge flow type on the plane A′B′ which is resulted from inlet flows through the planes AA′ and BB′ is approximately symmetric with respect to the plane $z=0$. Solid lines indicate the weighted mean velocity distributions of the three lines on the each plane. The weight used here is number ratio of pictures of the discharge, upward and downward flow types. The velocity distribution around the impeller was also measured by LDV equipped with a frequency shifter. Simple ensemble average velocity for ten minutes for one measuring point is plotted in the figure on circle mark. The experimental accuracy of the data estimated from visualization can be examined by comparing the solid lines with LDV data. Agreement between them is good on the AA′ and BB′ planes. On the other hand, a difference is observed on the distributions on A′B′ plane. More data are required to obtain a real average distribution on the A′B′ plane. However, figure even suggests that the discharge stream through the plane A′B′ consists of quite different types of flow which replace one after another and suggests that a peculiar conditional sampling technique on LDV data processing is necessary to develope in order to obtain the nature of the flow.

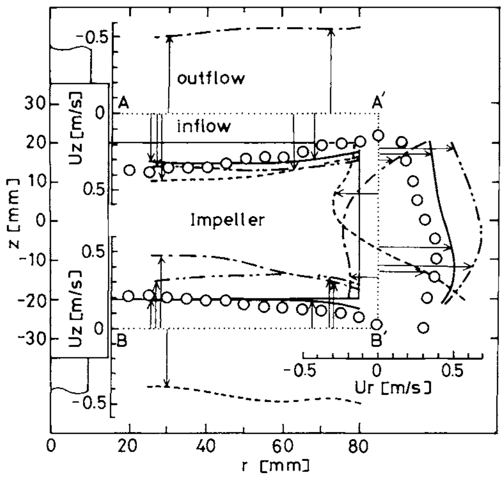

Fig. 4. Velocity distributions calculated from video pictures and measured by LDV; *Visualization*: two-dotted and dashed lines—Discharge patterns (TD & WD); dotted and dashed lines—Upward Cross-pass patterns (TP & WP) plus Asymmetric Discharge pattern (UD); dashed lines—Downward Cross-pass patterns (TP & WP) plus Asymmetric Discharge pattern (UD); solid lines—Weighted mean. *LDV*: mark ○

2.3 Flow field in the entire vessel

Flow in the whole vessel is more complicated to that in the impeller region. For examples, it is well known that vertical vortexes often appear and disappear behind the baffle edges, around the impeller shaft and on the liquid surface. The reverse flow to the usual flow direction of the circulation flow in the regions far from the impeller is also often found. Among the complicated flow phenomena, only simple phenomenon that is estimated to be significant is as follows. When discharge pattern taking place in the impeller region, flow in the vessel is very irregular in general. This can be seen on the movements of tracer particles as illustrated in **Fig. 5(a)**. In contrast, when flow in the impeller regions changes to the cross-pass pattern and developes in the entire impeller region, the flow throughout the vessel also immediately changes to a relatively simple profile. Figure 5(b) shows an illustration of the profile. **Figure 6** is a schematic profile of the flow summarized from the similar figures as shown in Fig. 5(b). The figure indicates that the flow after passing through a certain part of the impeller region often passes through again in the opposite side of the impeller region. The horizontal figure-eight loop was repeated to form a main flow. Sometimes the tracer particles enter the induced-flow region near the bottom as indicated in Fig. 6.

It is quite interesting that over 60% of the flow in the impeller region is occupied by the discharge flow

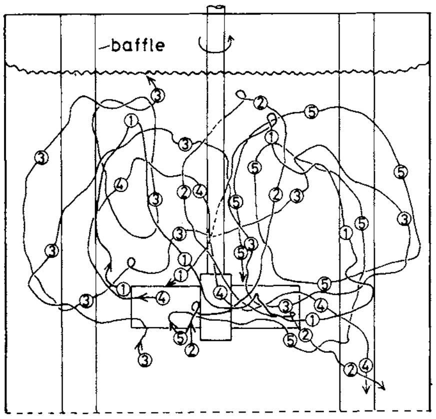

Fig. 5(a). Illustration of particle movements when pattern TD is taking place in the whole impeller region; numbers in the figure correspond to respective tracers

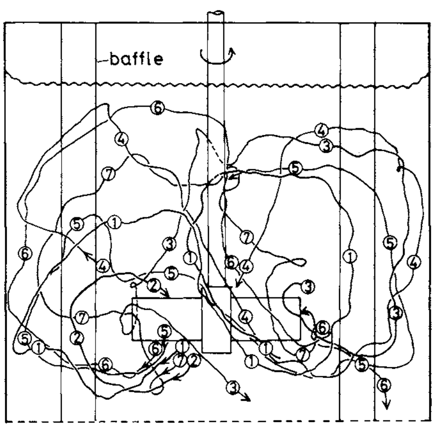

Fig. 5(b). Illustration of relatively simple circulation flow profiles when cross-pass pattern is predominant in the impeller region

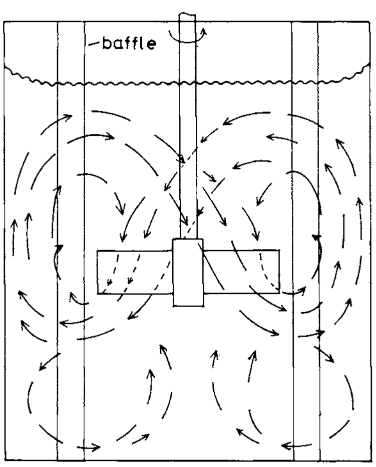

Fig. 6. Schematic flow profile at the cross-pass pattern taking place in the impeller region

patterns, accompanied by a complicated irregular motion in the vessel with high power consumption.

2.4 The wide fluctuation of torque

The estimation given above suggests that higher torque and lower torque, corresponding respectively to the typical discharge and typical cross-pass patterns, should appear repeatedly with very low frequency in the torque signal. An illustration is given in

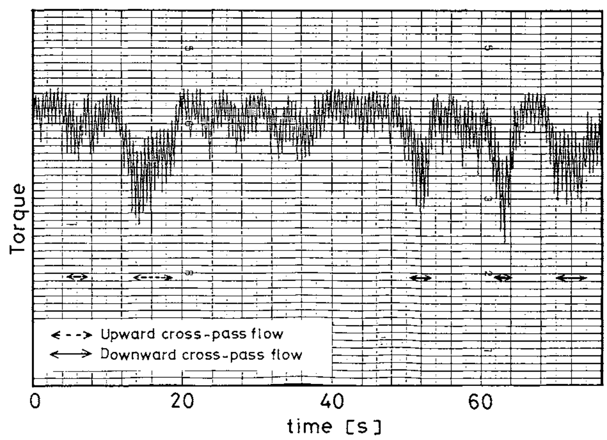

Fig. 7. Illustration of torque fluctuation

Table 2. Possibilities simultaneous occurrence of pattern combinations in the impeller region

	Combination	Lifetime ratio
(I)	TD-TD-TD-TD	9.3%
	TD-TD-TD-WD	12.5%
	TD-TD-UD-WD	4.9%
	TD-TD-WD-WD	11.4%
	TD-UD-WD-WD	4.5%
	TD-WD-WD-WD	6.4%
	Other combinations of TD, UD and WD	13.0%
	Total	62.0%
(II)	TP-TP-TP-TP	0.6%
	TP-TP-TP-WP	2.4%
	TP-TP-WP-WP	4.3%
	TP-WP-WP-WP	5.0%
	WP-WP-WP-WP	2.7%
	Total	15.0%
(III)	TD and others (not including TP)	3.0%
	UD and others (not including TP)	8.4%
	TP and others (not including TD and UD)	2.0%
	Total	13.4%
(IV)	Other combinations*	9.6%

* Combination of WD and WP, for example

Fig. 7. The periodic fluctuation in the figure corresponds to the impeller rotation. The result of simultaneous measurement and visualization is given in the figure for the cross-pass pattern (including WP). It is recognized from the figure that abrupt reduction of torque is always recorded when the cross-pass pattern has developed over the whole of the impeller region. However, it is hard to recognize whether the higher torque is caused by the higher discharge pattern or by the pattern combinations taking place in each space between blades. The latter pattern produces an unbalanced flow in the impeller region which should be accompanied by a relatively high level of torque. The total time ratio of the abrupt reduction of torque to the measurement time almost agreed with that of case (II) in **Table 2**. The cross-pass pattern is estimated

phenomenologically to be a kind of relaxation phenomenon, since only fluid having a large circumferential velocity at the inlet plane toward the impeller could pass through the impeller region axially. Therefore, it is expected that less agitation power should be consumed when cross-pass patterns are present.

Conclusions

The flow in and near the field of a paddle impeller can be characterized into five types of flow pattern, which are classified into discharge and the cross-pass flow types. The quite different patterns and their various combinations occurring repeatedly in the impeller region cause unusual large-scale fluctuations of flow in space and time near the field of the impeller.

When the cross-pass pattern had developed over the whole region between blades, a horizontal figure-eight pattern of flow also developed in the entire vessel with abrupt reduction of torque.

Literature Cited

1) Chang, T.P.K., Y. H. E. Sheu, G. B. Tatterson and D. S. Dickey: *Chem. Eng. Commun.*, **10**, 21 (1981).
2) Cutter, L. A.: *AIChE J.*, **12**, 35 (1966).
3) Gunkel, A. A. and M. E. Weber: *AIChE J.*, **21**, 931 (1975).
4) Kim, W. J. and F. S. Manning: *AIChE J.*, **10**, 747 (1964).
5) Mochizuki, M. and I. Takashima: *Kagaku Kogaku Ronbunshu*, **8**, 487 (1982).
6) Mochizuki, M. and I. Takashima: *Kagaku Kogaku Ronbunshu*, **30**, 539 (1984).
7) Mujumdar, A. S., B. Huang, D. Wolf, M. E. Weber and W. J. M. Douglas: *Can. J. Chem. Eng.*, **48**, 475 (1975).
8) Nagase, Y., T. Iwamoto, S. Fujita and T. Yoshida: *Kagaku*, **38**, 519 (1974).
9) Nagase, Y.: '77 Mixing Conference preprint, New Hampshire, U.S.A. (1977).
10) Nagase, Y.: "Fluid Mixing Chem. Eng. Symposium series 6," p. 72, in Japanese (1984).
11) Nagase, Y.: "Note on Mixing," Shimazaki Mixing Eq. Co. Ltd. (1986).
12) Oldshue, J. Y.: Fluid Mixing Technology, Chem. Eng., McGraw Hill Pub. (1983).
13) Rao, A. M. and R. S. Brodkey: *Chem. Eng. Sci.*, **27**, 13 (1972).
14) Sato, Y., M. Kamiwano and K. Yamamoto: *Kagaku Kōgaku*, **34**, 104 (1974).
15) van der Molen, K. and H. R. E. van Mannen: *Chem. Eng. Sci.*, **33**, 1161 (1978).
16) van't Riet, K. and J. M. Smith: *Chem. Eng. Sci.*, **28**, 1031 (1973).
17) van't Riet, K., W. Bruijn and J. M. Smith: *Chem. Eng. Sci.*, **31**, 407 (1976).
18) Yianneskis, M., Z. Popiolek and J. H. Whitelaw: *J. Fluid Mech.*, **175**, 537 (1987).